СТРОИТЕЛЬНАЯ МЕХАНИКА ИНЖЕНЕРНЫХ КОНСТРУКЦИЙ И СООРУЖЕНИЙ
STRUCTURAL MECHANICS OF ENGINEERING CONSTRUCTIONS AND BUILDINGS

2024. 20(6). 552–566

ISSN 1815-5235 (Print), 2587-8700 (Online)
HTTP://JOURNALS.RUDN.RU/STRUCTURAL-MECHANICS

ПРОБЛЕМЫ ТЕОРИИ УПРУГОСТИ
PROBLEMS OF THEORY OF ELASTICITY

DOI: 10.22363/1815-5235-2024-20-6-552-566
UDC 539.42
EDN: CXIPEP

Research article / Научная статья

Specific Strength Under Combined Loading

Arslan K. Kurbanmagomedov[1] ✉, **Evgeny M. Morozov**[2]

[1] RUDN University, *Moscow, Russia*
[2] Department of Density Physics, National Research Nuclear University MEPhI, *Moscow, Russia*
✉ kurbanmagomedov_ak@pfur.ru

Received: September 10, 2024
Accepted: November 11, 2024

Abstract. The work is devoted to the application of the concept of specific strength for the analysis of the degree of utilization of mechanical properties of beam material under combined loading. The beam is studied and force diagrams are constructed for various types of loads, such as pure bending with tension, pure bending with tension and torsion, pure bending with torsion, and the strength utilization factor of a beam with an arbitrary cross-section is obtained. The research method is based on the superposition of stress states with the determination of the difference between the resistance diagrams. The concept of material resistance to fracture in the form of ultimate stresses distributed over the body volume is introduced. The method of calculating the specific strength for a beam under combined stress, as well as for thick-walled pipes loaded with internal pressure, is given. The relationship between the beam cross-section of the beam and the specific strength is presented, followed by a conclusion for the optimal application of the beam with the cross-section used.

Keywords: fracture mechanics, solid mechanics, composite material, failure of solid materials and structures, deformation

Conflicts of interest. The authors declare that there is no conflict of interest.

Authors' contribution. *Kurbanmagomedov Arslan* — numerical analysis, evaluation of research results, preparation of text and infographics, final conclusions. *Morozov Evgeny* — research concept, development of methodology, final conclusions.

For citation: Kurbanmagomedov A.K., Morozov E.M. Specific strength under combined loading. *Structural Mechanics of Engineering Constructions and Buildings.* 2024;20(6):552–566. http://doi.org/10.22363/1815-5235-2024-20-6-552-566

Arslan K. Kurbanmagomedov, Candidate of Physical and Mathematical Sciences, senior lecturer, Nikolskii Mathematical Institute, RUDN University, Moscow, Russia; eLIBRARY SPIN-code: 5262-5269, ORCID 0000-0001-9158-0378; e-mail: kurbanmagomedov_ak@pfur.ru

Evgeny M. Morozov, Doctor of Technical Sciences, Professor, National Research Nuclear University MEPhI (Moscow Engineering Physics Institute) Moscow, Russia; eLIBRARY SPIN-code: 3989-2934, ORCID: 0000-0002-4824-8481; e-mail: evgeny.morozof@gmail.com

Удельная прочность при сложном сопротивлении

А.К. Курбанмагомедов[1]✉, Е.М. Морозов[2]

[1] Российский университет дружбы народов, *Москва, Россия*
[2] Национальный исследовательский ядерный университет МИФИ, *Москва, Россия*
✉ kurbanmagomedov_ak@pfur.ru

Поступила в редакцию: 10 сентября 2024 г.
Принята к публикации: 11 ноября 2024 г

Аннотация. Исследовано применение понятия удельной прочности для расчетного изучения степени использования механических свойств материала бруса при его работе в условиях сложного сопротивления. Представлено исследование бруса с дальнейшим построением эпюр с различными видами нагрузок, таких как чистый изгиб с растяжением, чистый изгиб с растяжением и кручением, чистый изгиб с кручением и получен коэффициент использования несущей способности бруса с произвольным поперечным сечением. Метод исследования основан на суперпозиции напряженных состояний с определением различия между эпюрами сопротивления нагружению. Введено понятие сопротивления материала разрушению в виде предельных напряжений, распределенных по объему тела. Приведен метод расчета удельной прочности для сложнонапряженного бруса, а также толстостенных труб, нагруженных внутренним давлением. Представлена зависимость сечения бруса от удельной прочности, с последующим выводом для наиболее выгодного использования бруса с используемым сечением.

Ключевые слова: механика твердого тела, композиционный материал, разрушения твердых материалов и конструкций, деформация

Заявление о конфликте интересов. Авторы заявляют об отсутствии конфликта интересов.

Вклад авторов. *Морозов Е.М.* — научное руководство, концепция, развитие методологии, итоговые выводы. *Курбанмагомедов А.К* — анализ результатов исследования, подготовка исходного текста, подготовка инфографиков, итоговые выводы.

Для цитирования: *Kurbanmagomedov A.K., Morozov E.M.* Specific strength under combined loading // Строительная механика инженерных конструкций и сооружений. 2024. Т. 20. № 6. С. 552–566. http://doi.org/10.22363/1815-5235-2024-20-6-552-566

1. Introduction

Solving the problem of increasing strength of structures while simultaneously reducing weight and with minimal consumption of scarce materials leads to the development of methods for evaluating the degree of utilization of the shape and dimensions of the body and the strength of the material. These methods were developed first along the path of assessing the shape and dimensions of the cross-section [1–6] at a constant distribution of material properties across the cross-section. To create a body of equal strength in all its zones and in all directions, it is necessary to evaluate the degree of approximation to an equal-strength state and the correspondence of the stress state in each element of the body to the material strength in the same element.

Since in most cases material properties are distributed non-uniformly over the cross-section, either as a result of technological side processes or as a result of their deliberate changes, evaluation of the load-bearing capacity of the body must be made taking into account the variability of mechanical properties across the cross-sections of the body. Reasonable use and creation of variability in material properties plays a similar role to the rational choice of body shape. Recently, methods have been proposed for estimating the load-bearing capacity of bodies taking into account the variability of not only the stress distribution, but also the resistance distribution [2; 7; 8].

Курбанмагомедов Арслан Курбанмагомедович, кандидат физико-математических наук, старший преподаватель математического института С.М. Никольского, Российский университет дружбы народов, Москва, Россия; eLIBRARY SPIN-код: 5262-5269, ORCID: 0000-0001-9158-0378; e-mail: kurbanmagomedov_ak@pfur.ru

Морозов Евгений Михайлович, доктор технических наук, профессор, профессор кафедры физики прочности, Национальный исследовательский ядерный университет МИФИ, Москва, Россия; eLIBRARY SPIN-код: 3989-2934, ORCID: 0000-0002-4824-8481; e-mail: evgeny.morozof@gmail.com

In works [7–9] the main conclusion was that from the point of view of increasing the specific strength, it is not the stress distribution itself that is important, but the mutual correspondence of the stress and resistance distributions, and it is necessary to add the analysis of the stress distribution to the analysis of the resistance distribution.

2. Methods

Attempts to assess the load-bearing capacity of bodies and individual cross-sections have been made for the simplest loading cases — tension, pure bending, torsion. The bearing capacity of cross-sections is evaluated by specific strength [9–11] using a nondimensional coefficient θ_C, called the strength utilization factor, which varies from 0 to 1. Specific strength is numerically characterized by coefficient θ_C.

$$\theta_C = \frac{\int_F \sigma \ ydF}{\int_F \sigma_c y_{\max} dF} = \frac{M}{y_{\max} F \sigma_{av}}, \tag{1}$$

where M is the load-bearing capacity of the cross-section; $y_{\max}$ is the half-height of cross-section; σ_{av} is the average reduced resistance of the cross section; F is the area of the cross-section under study.

In evaluation of the bearing capacity, the existing bearing capacity must be compared with the maximum possible one and, thus, the unused reserves are identified. The given formula (1) allows to evaluate the degree of utilization of the mechanical properties of the material and the geometry of the body based on the specific strength of the body, i.e. strength per unit cross-sectional area of the body, per unit "arm" and per unit of average strength of the material.

The denominator in formula (1) represents the load-bearing capacity of some ideal cross-section, the entire area F of which is concentrated at the end of the "arm" $y_{\max}$, and the material of which has an average resistance of σ_{av}.

Based on this, it can be said that the specific strength of a body is the ratio of the bearing capacity of the body to the bearing capacity of an ideal body with the same dimensions. An ideal body (cross-section) has an average resistance, i.e. resistance equal to

$$\sigma_{av} = \frac{1}{F}\int_F \sigma_c dF, \tag{2}$$

where σ_c is the reduced resistance of the material of the cross-section, depending on the coordinates of the cross-section points. The reduced resistance based on the most common theories of strength (first and third) is either the resistance to brittle fracture, or the yield strength, or variable resistance to plastic deformation if hardening is taken into account.

Thus, specific strength (similar to efficiency) is a dimensionless number varying from 0 to 1. A specific strength value equal to one (achieved only in rare cases) corresponds to 100% utilization of the given dimensions and strength of the material.

Below is an attempt to calculate the specific strength value for combined loading cases for a straight beam.

In the general case, the internal forces in the given section of a beam form the resultant vector and the resultant moment [11; 12], which can be decomposed into the following components (Figure 1). The resultant moment is decomposed into two components: perpendicular to the cross-section plane, M_T (torque moment), and lying in the section plane, M_B (bending moment). The resultant vector — into force *P* perpendicular to the cross-section (applied at the center of gravity of the cross-section) and the shear force, which is not taken into account.

An ideal section can be represented as two concentrated areas F_i spaced from each other at the maximum possible distance h (dimension) perpendicular to the M_B vector (Figure 1). This type of cross-section is ideal for bending moment apprehension. For torsion resistance, a thin-walled ring of diameter h with area F_K is ideal. It is assumed that steady state is maintained for ideal sections. Both types of cross-sections are able to carry axial load. Thus, the ideal cross-section for a combined load is assumed to consist of the sum of two separate types of ideal cross-sections [13–15].

The load-bearing capacity of the real cross-section is determined by a set of values P, M_B, M_T, which satisfy the strength conditions (according to the chosen strength theory) with a certain reserved strength.

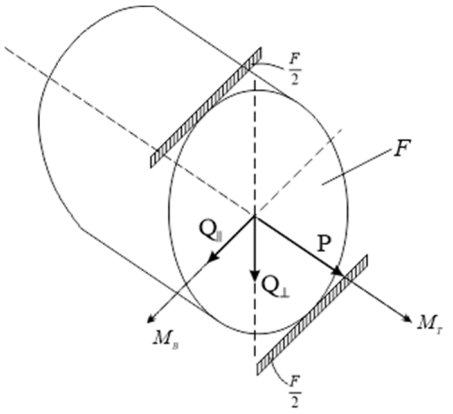

Figure 1. Two types of ideal cross sections
S o u r c e: made by A.K. Kurbanmagomedov

In order to ensure that the specified load acting on the real cross-section can also be accepted by the ideal cross-section, it is necessary to find the values of the areas F_i and F_K of the ideal cross-section. The required areas F_i and F_K can be found from the strength conditions for both types of ideal cross-sections.

For the part of the ideal cross-section subjected to bending and axial load, the following is obtained:

$$\sigma_{\text{av}} = \frac{P}{F_i + F_K} + \frac{2M_B}{hF_i}. \tag{3}$$

For the annular part of an ideal cross-section, subjected to torsion and axial load, the following is obtained:

- according to the 1-st theory of strength

$$2\sigma_{\text{av}} = \frac{P}{F_i + F_K} + \sqrt{\left(\frac{P}{F_i + F_K}\right)^2 + 4\left(\frac{2M_T}{hF_K}\right)^2}, \tag{4}$$

- according to the 3-rd theory of strength

$$\sigma_{\text{av}}{}^2 = \left(\frac{P}{F_i + F_K}\right)^2 + 4\left(\frac{2M_T}{hF_K}\right)^2. \tag{5}$$

The presented equations determine the minimum required areas for carrying maximum loads P, M_B, M_T. With such values of the areas of the ideal cross-section, loads P, M_B, M_T will be ultimate not only for the given cross-section, but also for the ideal cross-section. The sum of areas $F_i + F_K$ gives the total area of the ideal cross-section required to carry the ultimate sum of all types of loads. Moreover, each of the two areas resists with ultimate efficiency only to its own type of load [16–19]. The total area of the ideal cross-section is less than (or equal to) the area of the given cross-section. To assess the degree of utilization of the material properties and the shape of the cross-section, the ratio of the areas can be taken: the minimum area required to withstand the specified combined ultimate load, and the given area that carries the specified combined ultimate load. Then the coefficient evaluating the specific strength will be

$$\theta_C = \frac{F_i + F_K}{F}, \tag{6}$$

where F_i, F_K are the required values of ideal cross-sectional areas calculated using equations (3), (4) or (5).

Under the action of only one type of load, coefficient θ_S according to formula (6) coincides with the strength utilization factor (1) according to the work of N.D. Sobolev and Ya.B. Friedman [7–9].

In fact, substituting the value of the ultimate bending moment from (3) into (1) results in

$$\theta_C = \frac{M}{y_{\max} F \sigma_{\text{av}}} = \frac{F_i}{F}.$$

Thus, the ratio of the minimum required area to the given one evaluates the specific strength of the cross-section in the same way as the ratio of the load-bearing capacities. Specific strength in terms of bearing capacity under combined load can be characterized by the ratio of ray segments from the coordinate origin to the real and ideal ultimate load curves:

$$\theta_C = \frac{\sqrt{P^2 + M_i^2 + M_T^2}}{\sqrt{P^2 + M_i^2 + M_K^2}},$$

where the numerator is the ultimate load of the given cross-section, and the denominator is the ultimate load of the ideal cross-section, the area of which is equal to the area of the given cross-section.

However, this method must be abandoned, since adding values with different dimensions can lead to inconsistencies.

In formulas (3)–(5), there are maximum loads for the given cross-section, i.e. they satisfy the strength condition according to the maximum normal stress theory

$$2\sigma_{\text{c}} = \frac{P}{F} + \frac{M_B}{\mathcal{I}_Z} y + \sqrt{\left(\frac{P}{F} + \frac{M_B}{\mathcal{I}_Z} y\right)^2 + 4\tau^2}\ . \tag{7}$$

or the strength condition according to the maximum shear stress theory

$$\sigma_c = \sqrt{\left(\frac{P}{F} + \frac{M_B}{\mathcal{I}_Z} y\right)^2 + 4\tau^2}\ . \tag{8}$$

Here τ is the shear stress at the tangency point of the σ_c and σ diagrams.

The specific strength evaluated using the strength utilization factor (6) shows the degree of utilization of the cross-sectional shape and mechanical properties of the material.

As an example of specific strength calculation, some special cases of combined resistance are considered further.

2.1. Pure Bending with Tension

1. Let a beam have rectangular cross-section and constant material resistance. Bending moment M_B acts in the principal plane. Using the 3-rd theory of strength according to equation (8) for the given cross-section (rectangle), the following is obtained:

$$F\sigma_c = P + \frac{6}{h} M_B\,. \tag{9}$$

Substituting the loads from (9) into (3) and then into (5), the strength utilization factor is obtained:

$$\theta_C = \frac{P}{F\sigma_{\text{av}}} + \frac{2M_B}{hF\sigma_{\text{av}}} = 1 - \frac{4M_B}{hF\sigma_c}\,.$$

In Figure 2, the values of θ_C are plotted on the lines of ultimate forces and moments [1]. The specific strength of the body equal to 0.33 under bending increases linearly with the increase of ratio $\frac{P}{M_n}$ and becomes equal to one in the absence of bending.

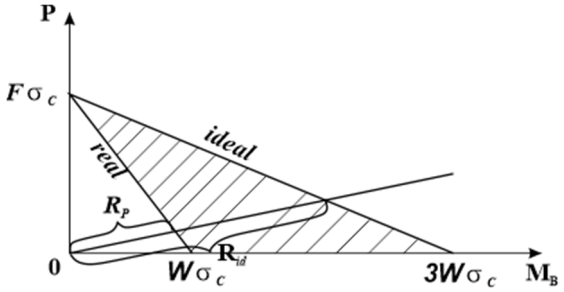

Figure 2. The combined effect of bending and stretching on the beam
S o u r c e : made by A.K. Kurbanmagomedov

2. Let the resistance increase linearly from $\frac{\sigma_c}{2}$ on the central axis to the value of σ_c at the upper and lower points of the rectangular cross-section. The average resistance in this case is equal to $\frac{3}{4}\sigma_c$.

Here, when calculating the strength, it is necessary to distinguish between three cases (Figure 3) depending on the points of the cross-section at which the σ and σ_c diagrams contact.

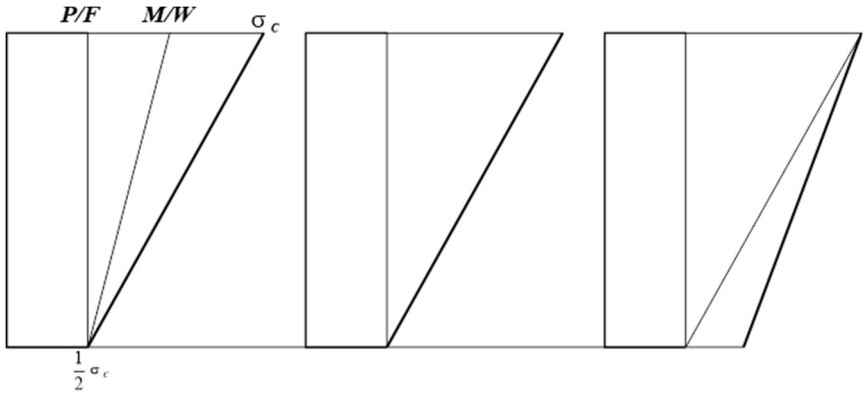

Figure 3. Stress and resistance diagrams for bending and stretching
S o u r c e: made by A.K. Kurbanmagomedov

From equation (8), the following is obtained:

$$F\sigma_c = P + 6\frac{M}{h}, \tag{10}$$

where for the above three cases the loads are limited as follows:

Case I	Case 2	Case 3
$P = \frac{1}{2}F\sigma_c$	$P = \frac{1}{2}F\sigma_c$	$P < \frac{1}{2}F\sigma_c$
$M < \frac{1}{2}W\sigma_c$	$W = \frac{1}{2}W\sigma_c$	$M > \frac{1}{2}W\sigma_c$

The strength utilization factor is obtained from (6) by substituting the loads from (10) into (3):

$$\theta_C = \frac{4}{3}\frac{P}{F\sigma_c} + \frac{8}{3}\frac{M}{hF\sigma_c}.$$

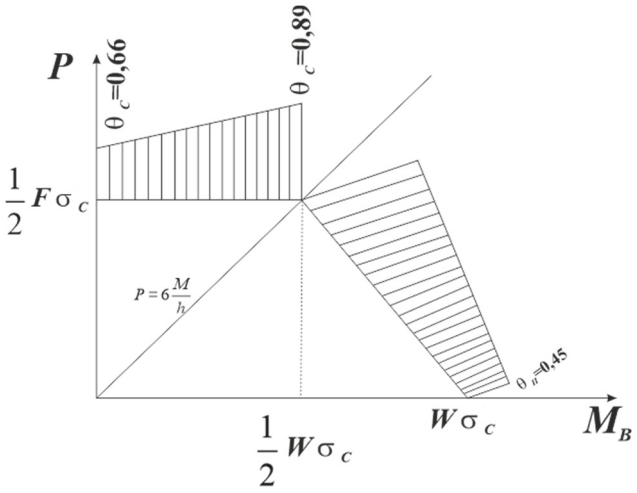

Figure 4. The strength utilization factor under combined bending and stretching of the beam
S o u r c e: made by A.K. Kurbanmagomedov

In Figure 4, strength utilization factor θ_C is plotted on the line of ultimate loads P and M_B. At a value of $P = 6\dfrac{M}{h}$ the specific strength is the highest due to the coincidence of σ and σ_C curves. In tension only, the specific strength decreases to 0.66, and in bending only to 0.45.

In Figure 4, strength utilization factor θ_C is plotted on the line of ultimate loads P and M_B. At a value of $P = 6\dfrac{M}{h}$ the specific strength is the highest due to the coincidence of σ and σ_C curves. In tension only, the specific strength decreases to 0.66, and in bending only to 0.45.

2.2. Tension with Pure Bending and Torsion

3. Let the cross-section be round with constant resistance.
For such a cross-section, the following is obtained from (8):

$$\left(F\sigma_c\right)^2 = \left(P + 8\frac{M_B}{d}\right)^2 + 64\left(\frac{M_T}{d}\right)^2.$$

Substituting these load values into formulas (3) and (5) and then into (6), the load-bearing capacity coefficient is obtained, which is plotted for the values of the ultimate loads corresponding to the coordinate planes (Figure 5).

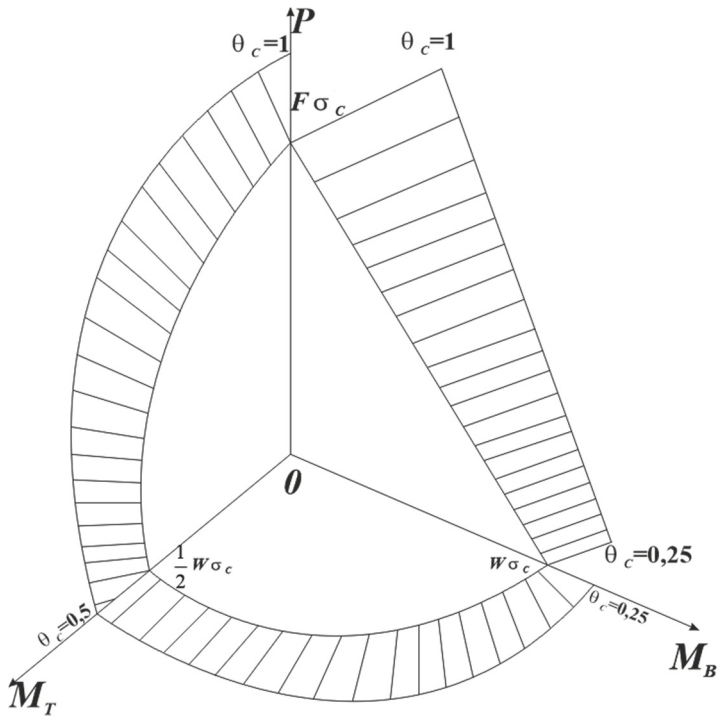

Figure 5. The combined effect of stretching, torsion and bending on the beam
S o u r c e: made by A.K. Kurbanmagomedov

4. Let the same beam have variable resistance of the cross-sectional material. At the center of the round cross-section the resistance is equal to $\frac{\sigma_c}{2}$. The resistance increases linearly along the radius to the value of σ_C at the circumference. The average cross-sectional resistance according to (2) is equal to $\frac{5\sigma_c}{6}$.

The point of contact of diagrams σ and σ_C will be in the center of the circle at

$$\frac{P}{F}=\frac{\sigma_c}{2};\ n\left(F\sigma_c\right)^2>\left(P+8\frac{M_B}{d}\right)^2+64\left(\frac{M_T}{d}\right)^2.$$

Contact of σ and σ_C will occur on the surface if

$$\frac{P}{F}<\frac{\sigma_c}{2};\ \sigma_c{}^2=\left(\frac{P}{F}+\frac{M_B}{W}\right)^2+4\left(\frac{M_{kT}}{W_p}\right)^2.$$

If the stress and resistance diagrams contact simultaneously both in the center and on the surface, then

$$\sigma_c{}^2=\left(\frac{\sigma_c}{2}+\frac{M_B}{W}\right)^2+4\left(\frac{M_T}{W_p}\right)^2.$$

Based on these cases, Figure 6 shows the surface of ultimate *P, M_B, M_T* and the strength utilization factor. The most favorable load ratios are determined by the greatest mutual approach of the σ and σ_C diagrams, at which the specific strength is the highest [17–20].

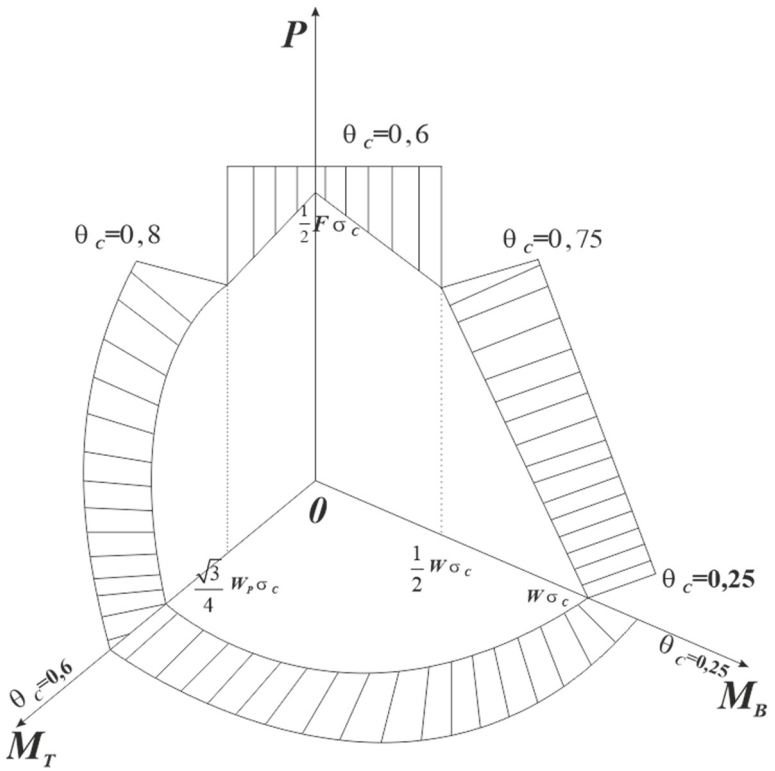

Figure 6. Cross-section of regions on coordinate planes
S o u r c e: made by A.K. Kurbanmagomedov

2.3. Pure Bending with Torsion

5. Let the cross-section be elliptical with constant resistance. The bending moment acts in the plane of the major axis of the ellipse. When the reduced stress at the end points of the major axis of the ellipse reaches the resistance value, the load-bearing capacity of the section will be exhausted and according to (8)

$$\frac{a^2}{16}F^2\sigma_c{}^2 = M_B^2 + M_T^2.$$

In this respect, there are three possible cases:

I.	II.	III.
$M_T = \frac{\pi ab^2}{4}\sigma_c$	$M_T = \frac{\pi ab^2}{4}\sigma_c$	$M_T < \frac{\pi ab^2}{4}\sigma_c$
$M_B < \frac{F\sigma_c}{4}\sqrt{a^2-b^2}$	$M_B = \frac{F\sigma_c}{4}\sqrt{a^2-b^2}$	$M_B > \frac{F\sigma_c}{4}\sqrt{a^2-b^2}$

In case 1, σ touches σ_C at the extreme points of the minor axis of the ellipse (with that $a < b$); in case 3 — at the extreme points of the major axis of the ellipse ($a > b$); in case II ($a = b$) — simultaneously at both of these and other points of the cross-section.

Plotting strength utilization factor on the curves of the ultimate M_B and M_T (Figure 7), it can be observed that the specific strength depends on the ratio of semi-axes of the ellipse and with an increase in the proportion of torque it varies from 0.25 to 0.5 $\frac{b}{a}$.

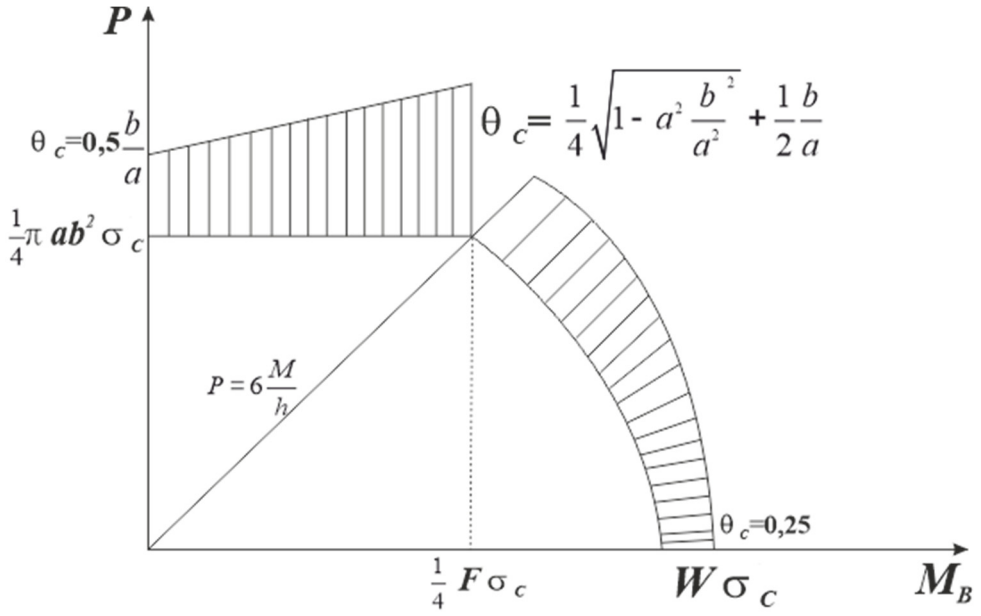

Figure 7. The strength utilization factor in case of combined torsion and bending
S o u r c e: made by A.K. Kurbanmagomedov

For a particular ratio between bending and torque ultimate moments, the most favorable ratios of ellipse semi-axes can be found. For example, for case II, equating the derivative of θ_C in terms of $\frac{b}{a}$ to zero, the most favorable cross-sectional shape is obtained at $\frac{b}{a} = 0.89$.

Let the application of the concept of specific strength to the calculation of the optimal cross-section dimensions be demonstrated using a specific example.

Cantilever steel tubular shaft is subjected to static bending moment $M_B = Pl$ and torque $M_T = Pa$. The shaft has variable strength in the normal annular cross-section.

The outer layer of the shaft with a thickness of σ = 5 mm has a strength K times greater than the core (increasing the strength of the surface layers can be structurally achieved, for example, by freeze casting a stronger material onto the core).

The optimal value of the internal diameter d is determined assuming that the remaining parameters are specified and constant, and the violation of strength occurs in the subsurface layer of the shaft.

The following notation is adopted:

D = 30mm is the outer diameter of the shaft annular section;

σ_{sl}, σ_{sc} are the resistances (strengths) of the material of the surface layer and the shaft core respectively;

$$C = \frac{d}{D};\ \ h = \frac{\delta}{D} = 0.167;\ \ K = \frac{\sigma_{sl}}{\sigma_{sc}} = \frac{50}{30} = 1.66.$$

From (8), the ultimate value of the force is obtained as

$$P = \frac{\pi D^4 \left(1 - c^4\right)\sigma_{sc}}{32\left(D - 2\delta\right)\sqrt{l^2 + a^2}}.$$

The average resistance according to (2) will be

$$\sigma_{av} = \frac{4h\left(1-h\right)}{1-c^2}\left(\sigma_{sl} - \sigma_{sc}\right) + \sigma_{sc}.$$

Substituting P and σ_{av} into (3), (5) and (6), the strength utilization factor is obtained as

$$\theta_C = \frac{\left(l + 2a\right)\left(1 - c^4\right)}{2\left(1-2h\right)\left[4h\left(1-h\right)\left(k-1\right) + \left(1-c^2\right)\right]\sqrt{l^2 + a^2}}.$$

From the condition of maximum specific strength of the cross-section $\frac{\partial \theta_C}{\partial c} = 0$, the equation for determining the best value of C is obtained:

$$c^4 - \left[8h\left(1-h\right)\left(k-1\right) + 2\right]c^2 + 1 = 0.$$

For the considered case, this results in C = 0.57, or the internal diameter should be equal to 17 mm.

2.4. Specific Strength of Thick-Walled Pipes

The specific strength of a beam under combined loading was discussed above. Let the definition of specific strength be applied to evaluate the extent to which the strength of thick-walled pipes loaded with internal pressure is utilized [21–23].

A thin-walled pipe is assumed to be an ideal body, based on obtaining the maximum load-bearing capacity for a given internal radius of the pipe, considering that the entire thickness of the thick-walled pipe under consideration is concentrated in its internal diameter. The resistance of the material of an ideal pipe, according to definition, is equal to the average resistance of the material of the given thick-walled pipe [23–26].

Then the reference load-bearing capacity of an ideal pipe will be:

$$P_{id} = \frac{\sigma_{av}\left(R-r\right)}{r},$$

where $\sigma_{av} = \dfrac{\int_r^R \sigma_c d\rho}{R-r}$ is average resistance.

The specific strength of a thick-walled pipe will be:

$$\theta_C = \frac{P}{P_{id}} = \frac{pr}{\sigma_{av}\left(R-r\right)},$$

where p is the load-bearing capacity of this pipe; *R, r* are the outer and inner radii of the thick-walled pipe under consideration.

The resulting coefficient can be represented as a product of the coefficients of equal strength and shape:

$$\theta_C = \frac{P}{P'}\frac{P'}{P_{id}} = \theta_p\theta_{sh},$$

where P' is the maximum internal pressure in the thick-walled pipe, in which the reduced stresses σ throughout the entire thickness of the pipe coincide with the σ_c resistance diagram.

3. Results and Discussions

The coincidence of the diagram of reduced stress from internal pressure with the resistance diagram can be achieved, for example, by continuously increasing the elastic modulus along the thickness of the pipe from the inner to the outer surface. The practical implementation of a continuous change in the elastic modulus according to the desired law is apparently difficult to achieve.

The specific strength calculated for some cases of resistance of thick-walled pipes is given in Table.

The Table shows that for a jointed pipe and for a pipe, part of the wall of which has crossed into the plastic zone, the strength utilization factor is approximately the same. In the case of a very thick pipe wall, the specific strength drops significantly, which indicates that pipes with very thick walls are unprofitable. By changing the diagram of the yield strength along the thickness of the pipe, it is possible to increase the strength utilization of the pipe yet in the elastic stage to the degree of utilization in case of plastic operation of the pipe with constant resistance.

Material specifications

Material	Temper	Chemical Composition	Physical Properties						Description and Application	Test by Laboratory	Receiving inspection
			Dimension	Tensile Strength Lbs/Sq.In. Min.	Yield Strength Lbs/Sq.In.Min.	Elongation Min.	Rockwell Hardness Number	Cold Bend Angele			
Cold Finished High Yellow Brass **Copper** – 65% **Zinc** – 35%	Hard	**Copper** – 64.50–67.50% **Zinc** – 32.09% **Lead** – 0.35% **Iron** – 0.06%	Cold Drawn Seamless Tubing All sizes	68.000	40.000	—	B75 to B85	90° around radius equal to thickness	• Good for flat work. • Suitable for ornamental plate or panel parts. • Used for Squirrel Cage rotor and rings.	None	Dimensions, Tolerances, Quality and Appearance
Cold drawn Seamless tubing high yellow brass **Copper** – 67.5% **Zinc** – 32% Lead – 0.5%	Light Anneal	**Copper –** 65.00–8.00% **Zinc** – 0.98% **Lead** – 0.80% **Iron** – 0.07% **Tin –**0.15%	Cold Drawn Seamless Tubing All sizes	45.000	18.000	25%	—	180° around Pin equal to $1-\frac{1}{2}$ times	• A 7.5 cm long piece of tubing, after being split lengthwise will withstand opening out flat without showing cracks or flaws. • Example of use: Coil spools when ends are to be spun over.	None	Dimensions, Tolerances, Quality and Appearance
Cold drawn Seamless tubing high yellow brass **Copper** – 67.5% **Zinc** – 32% **Lead** – 0.5%	Half hard	**Copper** – 65.00–68.00% **Zinc** – 30.98% **Lead** – 0.80% **Iron** – 0.07% **Tin** – 0.15%	Cold Drawn Seamless Tubing All sizes	Physical properties on all sizes not available. May be obtained on specific sizes when desired.					• Suitable for brass railings. Also coil spools when not spun over.	None	Dimensions, Tolerances, Quality and Appearance

S o u r c e: made by A.K. Kurbanmagomedov

4. Conclusion

The following conclusion is made based on the obtained results:

1. The paper provides a method for calculating the specific strength for a beam under combined loading, as well as for thick-walled pipes loaded with internal pressure.

References

1. Gordeeva G.V., Kurbanmagomedov A.K., Spitsov D.V. Strength control of concrete structures during the assessment of the residual life of buildings and structures of a hazardous production facility in the field of thermal power engineering. *System technologies.* 2022;4(45):73–86. (In Russ.) https://doi.org/10.55287/22275398_2022_4_73

2. Ignatiev V.A., Ignatiev A.V., Zhidelev A.V. *The mixed form of the finite element method in problems of structural mechanics.*Volgograd: VSUACE (VolgGASU) Publ.; 2006. (In Russ.) EDN: OWNUOH

3. Lepikhin A.M., Morozov E.M., Makhutov N.A., Leschenko V.V. Possibilities of Estimation of Fracture Probabilities and Allowable Sizes of Defects of Structural Elements According to the Criteria of Fracture Mechanics. *Inorganic Materials.* 2023;59:1524–1531. (In Russ.) https://doi.org/10.1134/S0020168523150074

4. Makhutov N.A., Moskvichev V.V., Morozov E.M., Shlyannikov V.N., Gadenin M.M., Yudina O.N., Fedorova E.N. The international and national researches of strength, integrity and safety of engineering systems. *Safety and emergencies problems.* 2020;(1):5–19. (In Russ.) https://doi.org/10.36535/0869-4176-2020-01-1

5. Moskvichev V.V., Makhutov N.A., Shokin Yu.I. et al. *Applied problems of structural strength and mechanics of destruction of technical systems*. Novosibirsk: Nauka Publ.; 2021. (In Russ.) https://doi.org/10.7868/978-5-02-038832-1

6. Arkadov G.V., Getman A.F., Usanov A.I. Development and Application of Technologies Maintenance of a Lifetime and Safety the NPP Components. *Proceedings of the 16th International Conference on Nuclear Engineering.* Orlando, Florida, USA. May 11–15, 2008;1:313–319. ASME. https://doi.org/10.1115/ICONE16-48904

7. Sobolev N.D., Bogdanovich K.P. *Mechanical properties of materials and fundamentals of strength physics*. Moscow: MEPhI Publ.; 1985. (In Russ.)

8. Friedman Ya.B. *Unified theory of strength of materials:* With a preface. Academician N.N. Davidenkov. All-Union Scientific Research Institute of Aviation Materials. Moscow: Oborongiz Publ.; 1943. (In Russ.)

9. Morozov E.M., Polak L.S., Fridman Y.B. Variational Principles in the Development of Cracks in Solids. *Soviet Physics Doklady.* 1964;9:394. (In Russ.)

10. Kurbanmagomedov A., Radzhabov Z., Okolnikova G. Investigation of Normal Fracture Cracks in an Infinite Elastic Medium. *Networked Control Systems for Connected and Automated Vehicles. NN 2022. Lecture Notes in Networks and Systems*. 2023;509:1407–1417. https://doi.org/10.1007/978-3-031-11058-0_142

11. Honeycombe R. Plastic Deformation of Metals. *Nature.* 1932. Vol. 129. https://doi.org/10.1038/129717b0

12. Zakharov M.N., Morozov E.M., Nasonov V.A. Assessing the risk of welding defects. *Russian Engineering Research.* 2015;35(11):846–849. https://doi.org/10.3103/S1068798X15110180

13. Kurbanmagomedov A.K., Radzhabov Z.R., Okolnikova G.E. Investigation of Normal Fracture Cracks in Elastic-Layer Materials. *NeuroQuantology.* 2022;20(8):6378–6384. http://doi.org/10.14704/nq.2022.20.8.NQ44661

14. Khazhinsky G.M. *Mechanics of small cracks in strength calculations of equipment and pipelines.* Moscow: Fizmatkniga Publ.; 2008. (In Russ.) ISBN 978-89155-171-8

15. Morozov E.M., Kurbanmagomedov A.K. Is it possible to determine the whole crack path at once. *Structural Mechanics of Engineering Constructions and Buildings*. 2024;20(4):364–373. http://doi.org/10.22363/1815-5235-2024-20-4-364-373

16. Gordeeva G.V., Kurbanmagomedov A.K., Spitsov D.V. Strength control of concrete structures during the assessment of the residual life of buildings and structures of a hazardous production facility in the field of thermal power engineering. *The System technologies.* 2022;4(45):73–86. http://doi.org/10.55287/22275398_2022_4_73

17. Carpinteri A., Brighenti R., Spagnoli A. Part-through cracks in pipes under cyclic bending. *Nuclear Engineering and Design.* 1998;185(1):1–14. https://doi.org/10.1016/S0029-5493(98)00189-7

18. Carpinteri A., Brighenti R., Spagnoli A. Fatigue growth simulation of part-through flaws in thick-walled pipes under rotary bending. *International Journal of Fatigue.* 2000:22(1):1–9. https://doi.org/10.1016/S0142-1123(99)00115-2

19. Musayev V.K. Mathematical Modeling of Explosive and Seismic Impacts on an Underground Structure. *Power Technology and Engineering.* 2024;57(6):875–881. https://doi.org/10.1007/s10749-024-01751-9

20. *Ghelichi R., Kamrin K.* Modeling growth paths of interacting crack pairs in elastic media. *Soft Matter*. 2015;(11): 7995–8012. https://doi.org/10.1039/c5sm01376c

21. *Nikhamkin M., Ilinykh A.* Low cycle fatigue and crack grow in powder nickel alloy under turbine disk wave form loading: Validation of damage accumulation model. *Applied Mechanics and* Materials. 2014;(467):312–316. https://doi.org/10.4028/www.scientific.net/AMM.467.312

22. Wang Q., Ren J.Q., Wu Y.K., Jiang P., Sun Z.J., Liu X.T. Comparative study of crack growth behaviors of fully-lamellar and bi-lamellar Ti-6Al-3Nb-2Zr-1Mo alloy. *Journal of Alloys and Compounds.* 2019;789:249–255. https://doi.org/10.1016/j.jallcom.2019.02.302

23. Kolesnikov Yu.V., Morozov E.M. *Mechanics of contact failure.* Moscow: LKI Publ.; 2007. (In Russ.) ISBN: 978-5-382-00268-2

24. Matvienko Y.G., Morozov E.M. Two basic approaches in a search of the crack propagation angle. *Fatigue and Fracture of Engineering Materials and Structures*. 2017;40(8):1191–1200. https://doi.org/10.1111/ffe.12583

25. Pook L.P. The linear elastic analysis of cracked bodies, crack paths and some practical crack path examples. *Engineering Fracture Mechanics.* 2016;167:2–19. https://doi.org/10.1016/j.engfracmech.2016.02.055

26. Dombrovskii Y.M., Stepanov M.S. Mechanisms of Intragrain Plastic Deformation in Steel Heating Process. *Metal Science and Heat Treatment.* 2024;(65):747–750. https://doi.org/10.1007/s11041-024-01000-w

Список литературы

1. *Гордеева Г.В., Курбанмагомедов А.К., Спицов Д.В.* Контроль прочности бетонных конструкций при проведении оценки остаточного ресурса зданий и сооружений опасного производственного объекта в сфере теплоэнергетики // Системные технологии. 2022. № 4 (45). С. 73–86. https://doi.org/10.55287/22275398_2022_4_73

2. *Игнатьев В.А., Игнатьев А.В., Жиделев А.В.* Смешанная форма метода конечных элементов в задачах строительной механики. Волгоград : Изд-во ВолгГАСУ, 2006. 172 с. EDN: OWNUOH

3. *Lepikhin A.M., Morozov E.M., Makhutov N.A., Leschenko V.V.* Possibilities of Estimation of Fracture Probabilities and Allowable Sizes of Defects of Structural Elements According to the Criteria of Fracture Mechanics // Inorganic Materials. 2023. Vol. 59. P. 1524–1531. https://doi.org/10.1134/S0020168523150074

4. *Махутов Н.А., Москвичев В.В., Морозов Е.М., Шлянников В.Н., Гаденин М.М., Юдина О.Н., Федорова Е.Н.* Международные и национальные исследования прочности, целостности и безопасности технических систем // Проблемы безопасности и чрезвычайных ситуаций. 2020. № 1. С. 5–19. https://doi.org/10.36535/0869-4176-2020-01-1

5. *Москвичев В.В., Махутов Н.А., Шокин Ю.И.* и др. Прикладные задачи конструкционной прочности и механики разрушения технических систем. Новосибирск : Наука, 2021. 796 с. https://doi.org/10.7868/978-5-02-038832-1

6. *Arkadov G.V., Getman A.F., Usanov A.I.* Development and Application of Technologies Maintenance of a Lifetime and Safety the NPP Components // Proceedings of the 16th International Conference on Nuclear Engineering. Orlando, Florida, USA. May 11–15, 2008. Vol. 1. P. 313–319. ASME. https://doi.org/10.1115/ICONE16-48904

7. *Соболев Н.Д., Богданович К.П.* Механические свойства материалов и основы физики прочности. Москва : МИФИ, 1985. 82 с.

8. *Фридман Я.Б.* Единая теория прочности материалов: с предисл. акад. Н.Н. Давиденкова / Всесоюзный научно-исследовательский институт авиационных материалов. Москва : Оборонгиз, 1943. 94 с.

9. *Морозов Е.М., Полак Л.С., Фридман Ю.Б.* О вариационных принципах развития трещин в твердых телах // Доклады Академии наук СССР. 1964. Т. 146. № 3. С. 537–540.

10. *Kurbanmagomedov A., Radzhabov Z., Okolnikova G.* Investigation of Normal Fracture Cracks in an Infinite Elastic Medium // Networked Control Systems for Connected and Automated Vehicles. NN 2022. Lecture Notes in Networks and Systems. 2023. Vol. 509. P. 1407–1417. https://doi.org/10.1007/978-3-031-11058-0_142

11. *Honeycombe R.* Plastic Deformation of Metals // Nature. 1932. Vol. 129. https://doi.org/10.1038/129717b0

12. *Zakharov M.N., Morozov E.M., Nasonov V.A.* Assessing the risk of welding defects // Russian Engineering Research. 2015. Vol. 35. P. 846–849. https://doi.org/10.3103/S1068798X15110180

13. *Kurbanmagomedov A.K., Radzhabov Z.R., Okolnikova G.E.* Investigation of Normal Fracture Cracks in Elastic-Layer Materials // NeuroQuantology. 2022. No. 20 (8). P. 6378–6384. http://doi.org/10.14704/nq.2022.20.8.NQ44661

14. *Хажинский Г.М.* Механика мелких трещин в расчетах прочности оборудования и трубопроводов. Москва : Физматкнига, 2008. 254 с. ISBN 978-89155-171-8

15. *Morozov E.M., Kurbanmagomedov A.K.* Is it possible to determine the whole crack path at once // Structural Mechanics of Engineering Constructions and Buildings. 2024. Vol. 20. No. 4. P. 364–373. http://doi.org/10.22363/1815-5235-2024-20-4-364-373

16. *Gordeeva G.V., Kurbanmagomedov A.K., Spitsov D.V.* Strength control of concrete structures during the assessment of the residual life of buildings and structures of a hazardous productionfacility in the field of thermal power engineering // The System technologies. 2022. № 4 (45). P. 73–86. https://doi.org/10.55287/22275398_2022_4_73

17. *Carpinteri A., Brighenti R., Spagnoli A.* Part-through cracks in pipes under cyclic bending // Nuclear Engineering and Design. 1998. Vol. 185. No. 1. P. 1–14. https://doi.org/10.1016/S0029-5493(98)00189-7

18. *Carpinteri A., Brighenti R., Spagnoli A.* Fatigue growth simulation of part-through flaws in thick-walled pipes under rotary bending // International Journal of Fatigue. 2000. Vol. 22. No. 1. P. 1–9. https://doi.org/10.1016/S0142-1123(99)00115-2

19. *Musayev V.K.* Mathematical modeling of explosive and seismic impacts on an underground structure // Power Technology and Engineering. 2024. Vol. 57. No. 6. P. 875–881. https://doi.org/10.1007/s10749-024-01751-9

20. *Ghelichi R., Kamrin K.* Modeling growth paths of interacting crack pairs in elastic media. *Soft Matter*. 2015;(11): 7995–8012. https://doi.org/10.1039/c5sm01376c

21. *Nikhamkin M., Ilinykh A.* Low cycle fatigue and crack grow in powder nickel alloy under turbine disk wave form loading: Validation of damage accumulation model // Applied Mechanics and Materials. 2014. Vol. 467. P. 312–316. https://doi.org/10.4028/www.scientific.net/AMM.467.312

22. *Wang Q., Ren J.Q., Wu Y.K., Jiang P., Sun Z.J., Liu X.T.* Comparative study of crack growth behaviors of fully-lamellar and bi-lamellar Ti-6Al-3Nb-2Zr-1Mo alloy // Journal of Alloys and Compounds. 2019. Vol. 789. P. 249–255. https://doi.org/10.1016/j.jallcom.2019.02.302

23. *Колесников Ю.В., Морозов Е.М.* Механика контактного разрушения. Москва : Изд-во ЛКИ, 2007. 224 с. ISBN 978-5-382-00268-2

24. *Matvienko Y.G., Morozov E.M.* Two basic approaches in a search of the crack propagation angle // Fatigue and Fracture of Engineering Materials and Structures. 2017. Vol. 40. No. 8. P. 1191–1200. https://doi.org/10.1111/ffe.12583

25. *Pook L.P.* The linear elastic analysis of cracked bodies, crack paths and some practical crack path examples // Engineering Fracture Mechanics. 2016. Vol. 167. P. 2–19. https://doi.org/10.1016/j.engfracmech.2016.02.055

26. *Dombrovskii Y.M., Stepanov M.S.* Mechanisms of Intragrain Plastic Deformation in Steel Heating Process // Metal Science and Heat Treatment. 2024. No. 65. P. 747–750. https://doi.org/10.1007/s11041-024-01000-w